

Controlling the work function of ZnO and the energy-level alignment at the interface to organic semiconductors with a molecular electron acceptor

Raphael Schlesinger,¹ Yong Xu,² Oliver T. Hofmann,² Stefanie Winkler,³ Johannes Frisch,¹ Jens Niederhausen,¹ Antje Vollmer,³ Sylke Blumstengel,¹ Fritz Henneberger,¹ Patrick Rinke,² Matthias Scheffler,² and Norbert Koch^{1,3}

¹*Institut für Physik, Humboldt-Universität zu Berlin, 12489 Berlin, Germany*

²*Fritz-Haber-Institut der Max-Planck-Gesellschaft, 14195 Berlin, Germany*

³*Helmholtz-Zentrum Berlin für Materialien und Energie GmbH- BESSY II, 12489 Berlin, Germany*

(Received 4 November 2012; published 22 April 2013)

We show that the work function (Φ) of ZnO can be increased by up to 2.8 eV by depositing the molecular electron acceptor 2,3,5,6-tetrafluoro-7,7,8,8-tetracyanoquinodimethane (F4TCNQ). On metals, already much smaller Φ increases involve significant charge transfer to F4TCNQ. No indication of negatively charged F4TCNQ on ZnO is found by photoemission spectroscopy. This fundamental difference is explained by a simple electrostatic model that identifies the bulk doping and band bending in ZnO as key parameters. Varying Φ of the inorganic semiconductor enables tuning the energy-level alignment at ZnO/organic semiconductor interfaces.

DOI: [10.1103/PhysRevB.87.155311](https://doi.org/10.1103/PhysRevB.87.155311)

PACS number(s): 73.20.At, 73.30.+y, 79.60.Dp

I. INTRODUCTION

Inorganic/organic semiconductor heterojunctions have opened up new opportunities for (opto-) electronic devices due to their potential for combining the favorable properties of two distinct material classes. Inorganic semiconductors, for instance, often exhibit high charge-carrier mobility, whereas, the organic counterparts contribute efficient light-matter coupling. Designing such hybrid heterojunctions with desired functionality, e.g., efficient charge-carrier transfer, requires control of the energy-level alignment at the interfaces.¹ The use of thin interlayers (often only submonolayer coverage) that introduce tailored interface dipoles (IDs) may be a pathway to solve this challenge.² Deposition of strong electron acceptor molecules, such as 2,3,5,6-tetrafluoro-7,7,8,8-tetracyanoquinodimethane [(F4TCNQ), the structure shown in the inset of Fig. 1(a)] on metals gives rise to a considerable work-function (Φ) increase, which significantly alters the level alignment towards an organic semiconductor on top and, therefore, the transport properties at the interface.²⁻⁴ On metals, the origin of the Φ increase upon F4TCNQ deposition is a hybridization between the electronic wave functions of the metal and the molecule, accompanied by a substantial electron transfer from the metal to the molecule and, as a consequence, a localized interface dipole moment.^{5,6} This charge transfer is mainly driven by the fact that the electron affinity of F4TCNQ films⁷ is higher than the ionization energy of the metal electrons at the Fermi level (E_F). This raises the question whether a similar mechanism could occur for F4TCNQ adsorbed on a (doped) inorganic semiconductor where the density of charge carriers at E_F is typically low and electron transfer to localized surface states might be accompanied by a spatially extended space-charge layer and band bending. For instance, changes in surface band bending and Φ induced by atmospheric small molecules adsorbed on ZnO surfaces have been assigned to interfacial charge transfer,⁸ however, without further quantification. Density functional theory calculations for physisorbed NO₂ on ZnO(2 $\bar{1}$ 10) predict a transfer of up to 0.2 electrons, but bulk doping and band bending were not included.⁹

In this paper, we investigate the energy-level alignment and interaction mechanism of F4TCNQ deposited on the two polar

ZnO surfaces, i.e., O-terminated (000 $\bar{1}$) and Zn-terminated (0001). With ultraviolet photoelectron spectroscopy (UPS), we find an extraordinarily large adsorption-induced Φ increase ($\Delta\Phi$) of up to 2.8 eV. However, neither noticeably filled molecular states at or near E_F in UPS nor the emergence of shifted core-level signals in x-ray photoelectron spectroscopy (XPS), indicative of molecular anion formation, are observed. This implies minute electron transfer to F4TCNQ in contrast to what was observed for the same molecule on metals for even smaller $\Delta\Phi$'s.^{5,6} We present a simple electrostatic model for the adsorption of acceptors on idealized semiconductor surfaces, which differentiates between the potential drop within the substrate due to the formation of a space-charge region (i.e., band bending $\Delta\Phi^{\text{BB}}$)¹⁰ and the electrostatic potential drop between the surface and the organic acceptor due to charge transfer (i.e., interface dipole $\Delta\Phi^{\text{ID}}$). This demonstrates that high $\Delta\Phi$ of semiconductors can be achieved even with extremely small charge transfer, which is considerably different for metals. Finally, we show that the energy-level alignment at a ZnO/organic semiconductor interface can, indeed, be modified with an F4TCNQ interlayer.

II. EXPERIMENTAL DETAILS

Photoemission experiments were performed at the storage ring BESSY II (Berlin) at beamline PM4, experimental station SurICat, in ultrahigh vacuum (UHV) with a base pressure of 2×10^{-10} mbar. Photoemission spectra were recorded at room temperature and in normal emission with an energy resolution of 120 meV. For the measurement of the secondary electron cutoff (SECO), the sample was biased at -10 V to clear the analyzer work function. The SECO position was determined from the intersection of two straight lines defined by the baseline and the linear region of the SECO spectrum slope; the error bar of this method is ± 50 meV. Photon energies were 35 eV for UPS/SECO and 610 eV for XPS. ZnO films were grown by molecular-beam epitaxy on sapphire films¹¹ and were cleaned after transfer through air to the photoemission setup by repeated cycles of Ar-ion sputtering and annealing to 400 °C. Cleanliness of the surfaces

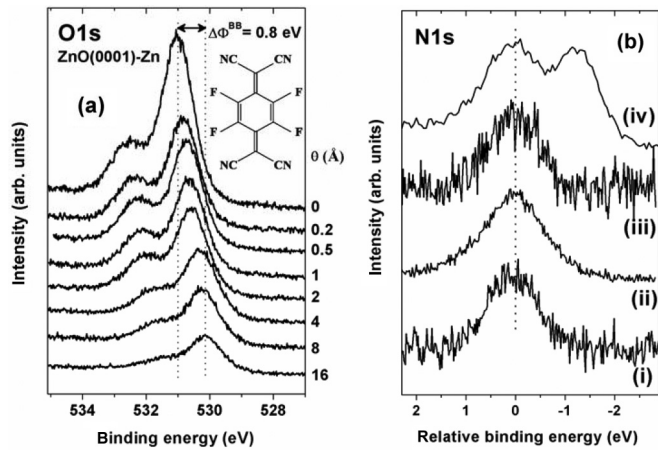


FIG. 1. (a) O1s core-level spectra for increasing F4TCNQ coverage (θ) on ZnO(0001)-Zn. (b) N1s core-level spectra of (i) 0.5-Å F4TCNQ on ZnO(0001), (ii) 8-Å F4TCNQ on ZnO(0001), (iii) 0.5-Å F4TCNQ on ZnO(000-1), and (iv) 60-Å F4TCNQ on Au (strong island growth). The spectra were shifted in binding energy to align the respective peak maxima for ZnO substrates with that for pristine F4TCNQ in multilayers on the Au substrate. The low-binding energy component in spectrum (iv) is from F4TCNQ chemisorbed on Au with a net electron transfer of approximately 0.3–0.4 eV (see text).

was verified by XPS by detecting only Zn and O core levels; no C core levels were observed, yielding (within our experimental limits) residual carbon contamination below 0.1 at.%. After conditioning in UHV, consistently $\sim 25\%$ of the surface oxygen atoms for both ZnO surfaces were bound to hydrogen as revealed by the high-binding energy component in the O1s core-level spectra [at 532.4 eV in Fig. 1(a) for pristine ZnO(0001)-Zn; for the ZnO(000 $\bar{1}$) surface and the peak fitting results for both surfaces, see Fig. S1 in the Supplemental Material.¹² This is consistent with previous theoretical and experimental work, which showed that, at room temperature, partial –OH termination of ZnO surfaces is thermodynamically stable.^{13–16} F4TCNQ (Sigma-Aldrich) was deposited from a resistively heated quartz crucible. The amount of evaporated material was monitored using a quartz crystal microbalance and was set to the rate equivalent of about

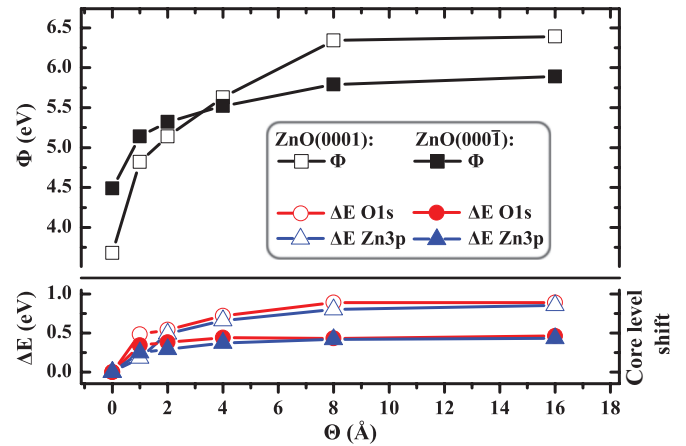


FIG. 3. (Color online) Evolution of the work function (Φ) as a function of F4TCNQ nominal thickness (Θ) on the ZnO(000 $\bar{1}$)-O and ZnO(0001)-Zn surfaces obtained from the UPS spectra shown in Fig. 1 and relative binding energy shifts ΔE of the O1s and Zn3p core levels upon adsorption of F4TCNQ inferred from the XPS spectra shown in Fig. 1 and the Supplemental Material.¹²

1-Å/min film mass thickness using a density of 1.64 g/cm³ and assuming the same sticking coefficient on the quartz and the ZnO surfaces.

III. RESULTS AND DISCUSSION

The ZnO samples we used were *n* doped (concentration 10^{17} – 10^{18} cm⁻³, E_F in the bulk is, thus, estimated to be ~ 200 meV below the conduction-band minimum) as also evidenced by E_F being close to (O terminated) or even slightly above (Zn terminated) the conduction-band minimum (CBM) in UPS of the clean surface (Fig. 2). Upon incremental deposition of F4TCNQ, the SECO shifts and yields an increase in Φ from 4.5 eV to Φ of 5.9 eV ($\Delta\Phi = 1.4$ eV) for ZnO(000 $\bar{1}$)-O and from $\Phi = 3.7$ eV to $\Phi' = 6.5$ eV for ZnO(0001)-Zn ($\Delta\Phi = 2.8$ eV). The saturated Φ' is reached at a nominal F4TCNQ mass thickness of 16 Å (see Fig. 3). In analogy to the Φ evolution observed when F4TCNQ is deposited on metals,^{5,6} we assign the mass thickness at which saturation of Φ is

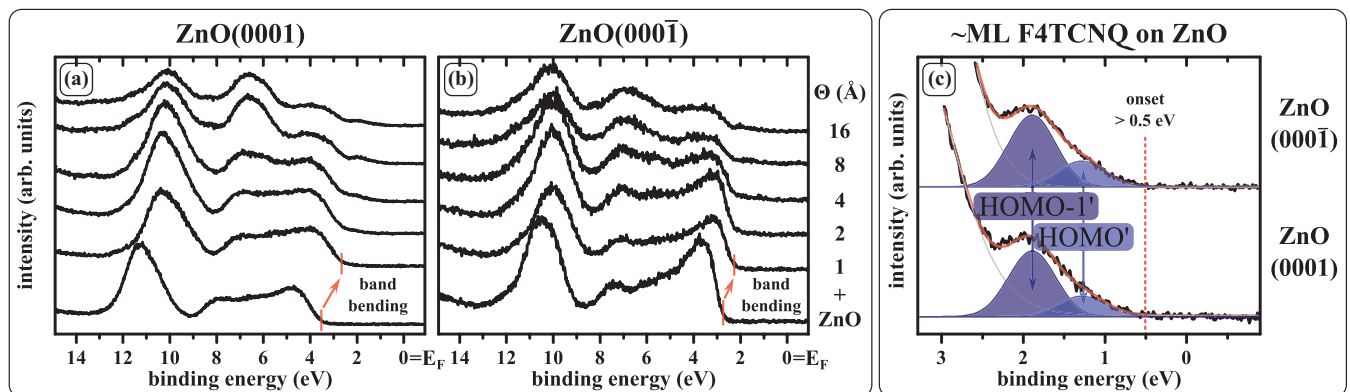


FIG. 2. (Color online) Valence region spectra of incrementally deposited F4TCNQ with nominal mass thickness (θ) on (a) ZnO(0001) and (b) ZnO(000 $\bar{1}$). In both graphs, the rigid shift in the ZnO valence band due to adsorption-induced surface band bending is indicated by arrows (for the lowest F4TCNQ θ). (c) Zoom of the valence spectra of about 1 monolayer (ML) F4TCNQ on ZnO. The frontier two peaks are assigned to be derived from the two highest occupied F4TCNQ levels.

achieved to correspond to the maximum F4TCNQ monolayer coverage (provided that molecules in multilayers do not further contribute to Φ changes); island growth of F4TCNQ may yet occur. The Φ increase is accompanied by a shift in the Zn3*p* and O1*s* core levels [exemplary spectra shown in Fig. 1(a); shifts summarized in Fig. 3] as well as the ZnO valence-band maximum to lower-binding energy (indicated in Fig. 2). All ZnO-derived levels shift in parallel by 0.5 eV on ZnO(000 $\bar{1}$)-O and by 0.8 eV on ZnO(0001)-Zn, which is indicative of a change in the ZnO surface band bending. The fact that core-level shifts (in XPS) and valence-band shifts (in UPS) occur in parallel evidences that surface photovoltage effects do not contribute to the observed energy-level shifts. Since the sample current (due to photoelectrons leaving the sample) in UPS was ~ 100 times lower than in XPS, surface charge accumulation is not an issue in our experiments. Therefore, $\Delta\Phi$ results from two phenomena: a change in surface band bending ($\Delta\Phi^{\text{BB}}$) (Ref. 12) in the inorganic semiconductor and the formation of a localized interface dipole ($\Delta\Phi^{\text{ID}}$) induced by the adsorption of the acceptor molecules onto ZnO. $\Delta\Phi^{\text{ID}}$ is, thus, 0.9 eV for ZnO(000 $\bar{1}$)-O and 2.0 eV for ZnO(0001)-Zn. The valence region (Fig. 2) exhibits F4TCNQ-derived photoemission features in the otherwise empty ZnO band gap. These consist of two peaks centered at 1.2 and 1.9 eV below E_F as shown in Fig. 2(c). In previous studies of F4TCNQ adsorbed on AlO_x, H-terminated diamond, graphene, and metals,^{5,17–20} F4TCNQ-derived peaks were observed as well but much closer to or even at E_F .^{5,18–20} These were assigned to be derived from the lowest unoccupied molecular orbital (LUMO) level—partially filled due to electron transfer from the substrate—and the relaxed highest occupied molecular orbital (HOMO) level of the F4TCNQ anion. However, in these studies, N1*s* core-level spectra gave evidence for highly negatively charged F4TCNQ due to the clear observation of a low-binding energy component (compared to pristine F4TCNQ). Such a component is absent for F4TCNQ adsorbed on ZnO. This is demonstrated in Fig. 1(b) with the N1*s* spectra of submonolayer and approximately monolayer F4TCNQ on both ZnO surfaces (only one peak visible) compared to that of F4TCNQ multilayer islands adsorbed on Au where both chemisorbed monolayer and pristine molecules in the multilayer are seen as two peaks separated by 1.3 eV. Note that the net charge transfer to F4TCNQ on Au is ~ 0.3 – 0.4 electrons per molecule.⁶ The apparently weak interaction of F4TCNQ with ZnO is further supported by the absence of any chemically shifted species in the Zn3*p* and O1*s* core-level spectra upon F4TCNQ adsorption (see Figs. 1, S1, and S2 in the Supplemental Material¹²). Furthermore, the core-level width stays virtually identical throughout the deposition sequence. This apparent discrepancy between the substantial $\Delta\Phi$, on the one hand, and the absence of telltale signs for large charge transfer on the other hand, i.e., notable chemically shifted N1*s* core levels and filled molecular states close to or at E_F , raises the question what mechanism is at work for F4TCNQ/ZnO.

To gain qualitative understanding of the experimental findings presented above, we consider a simple electrostatic model where electron transfer from the inorganic bulk to the molecules generates both band bending within the semiconductor as well as an interface dipole with an effective length

d_{eff} [see inset Fig. 4(a)]. Then, the total work-function change reads as

$$\Delta\Phi = \Delta\Phi_{\text{BB}} + \Delta\Phi_{\text{ID}}, \quad (1)$$

with the band-bending contribution in the Schottky-depletion-layer approximation,²¹

$$\Delta\Phi_{\text{BB}} = \frac{\delta q^2}{2\varepsilon_0\varepsilon N_D} \quad (2)$$

(ε_0 : vacuum permittivity, ε : static dielectric constant of the inorganic semiconductor, N_D : donor concentration in the inorganic semiconductor, and δq : area charge density on the acceptors) and

$$\Delta\Phi_{\text{ID}} = e \frac{\delta q}{\varepsilon_0} d_{\text{eff}} \quad (3)$$

(e : elementary charge). The (*a priori* unknown) d_{eff} between the charge on the molecular layer and the ZnO surface depends on the adsorption geometry of the molecule as well as on the exact definition of what constitutes the surfaces. In a reasonable estimate, d_{eff} is between 1 and 7 Å, an upper limit is the molecular length of about 10 Å. The area charge density δq adopted by the molecular layer is a function of $\Delta\Phi$ as well.²¹ Assuming that the LUMO can accept two electrons (of antiparallel spin) and ignoring, for simplicity, an energy difference in the single- and double-charged state, it holds that

$$\delta q = \frac{2eN_m}{e^{(E_{\text{LC}} + \Delta\Phi - E_F)/k_B T} + 1}, \quad (4)$$

where N_m is the area density of the molecular layer, E_{LC} is the energy separation between the LUMO level and the CBM at the surface, E_F is the Fermi level at doping concentration N_D measured relative to the position of the CBM in the bulk [which is used as zero of the energy scale in Eq. (4)], and $k_B T$ is the thermal energy. The solution of Eqs. (1)–(4), summarized in Fig. 4 with parameters adequate for the F4TCNQ/ZnO system, straightforwardly demonstrates the critical role of the inorganic semiconductor doping level. The work-function change scales, thus, with E_{LC} and is a smooth function of the donor concentration [Fig. 4(a)]. However, the charge transfer giving rise to $\Delta\Phi$ strongly changes with N_D [Fig. 4(b)]. For the ZnO-doping level used in our experiments (10^{17} – 10^{18} cm⁻³), the charge transferred per molecule hardly exceeds 0.02 electron, which is much below the charge occupation that can be resolved in the photoemission measurements. In this regime, the band-bending contribution $\Delta\Phi_{\text{BB}}$ dominates the total work-function change [Fig. 4(a)]. Lower carrier concentrations mean a more extended depletion layer width generating a larger potential change. At higher-doping levels, $\Delta\Phi$ only slightly increases [Fig. 4(a)], although substantial charge transfer is now required [Fig. 4(b)]. The situation is then reminiscent of that for a metal where the interface dipole alone determines the work-function change. The energy levels of ZnO before and after adsorption of F4TCNQ, including both contributions to $\Delta\Phi$, are summarized in Fig. 5.

Although the above considerations fully explain our experimental observation of large work-function changes but only minute charge transfer, a quantitative reproduction of the measured $\Delta\Phi$ values is beyond the simple electrostatic framework. A more detailed analysis requires, first, the

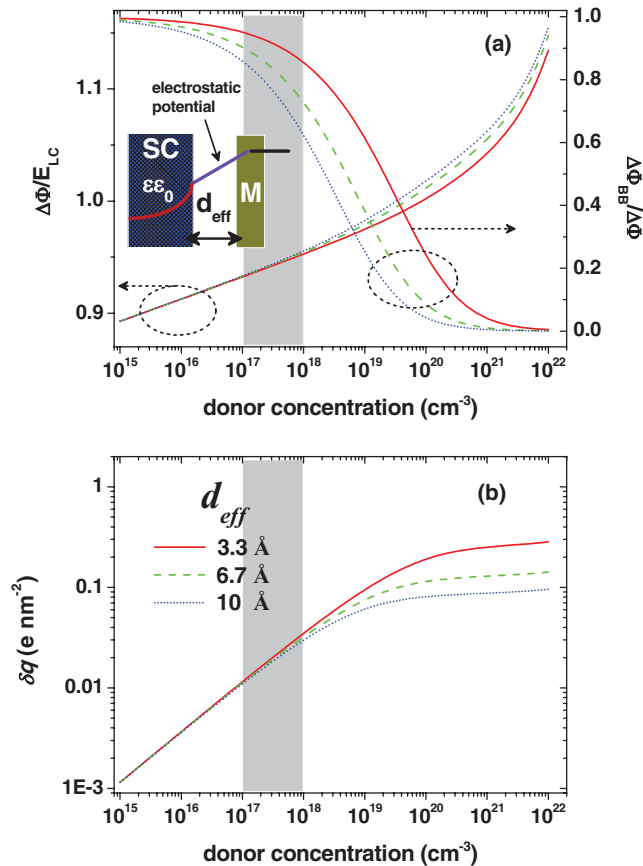


FIG. 4. (Color online) Molecular acceptor-induced work-function change and relative band-bending contribution to the total (a) work-function change and (b) charge transfer to the acceptor versus donor concentration in the inorganic semiconductor. Parameters used: $\epsilon = 9$, ZnO electron mass = 0.27, $N_m = 1 \text{ nm}^{-2}$, $E_{LC} = -1.5 \text{ eV}$, room temperature, and $d_{eff} = 3.3 \text{ \AA}$ (red), 6.7 \AA (green), and 10 \AA (blue). The shaded region indicates the doping level of ZnO in our experiments. The inset in (a) sketches the inorganic semiconductor (SC), the molecular acceptor (M), and the effective distance d_{eff} between the two.

detailed knowledge of the electronic structure of the molecule, of the ZnO surface, and of the adsorption induced changes. The latter also includes structural changes. For example, although F4TCNQ, as an inversion-symmetric molecule, bears no dipole moment of its own in the gas phase, structural changes (distortions upon adsorption, etc.) might induce such dipoles in addition to that produced by the charge transfer. This extra interface dipole depends on the molecular adsorption geometry and is likely different for the two ZnO surfaces studied here. Finally, we note that a space-charge layer is also present in the inorganic semiconductor prior to adsorption (Fig. 5). Thus, the “background charge” associated with this layer is a further parameter that will influence the specific work-function changes observed experimentally. In essence, a vertical shift in the curves displayed in Fig. 4(b), depending on the sign and magnitude of the background charge, would occur. Further experiments and electronic-structure calculations of the so far unknown adsorbate geometry, the surface and interface electronic density of states, and the electron transfer to resolve these issues are under way.

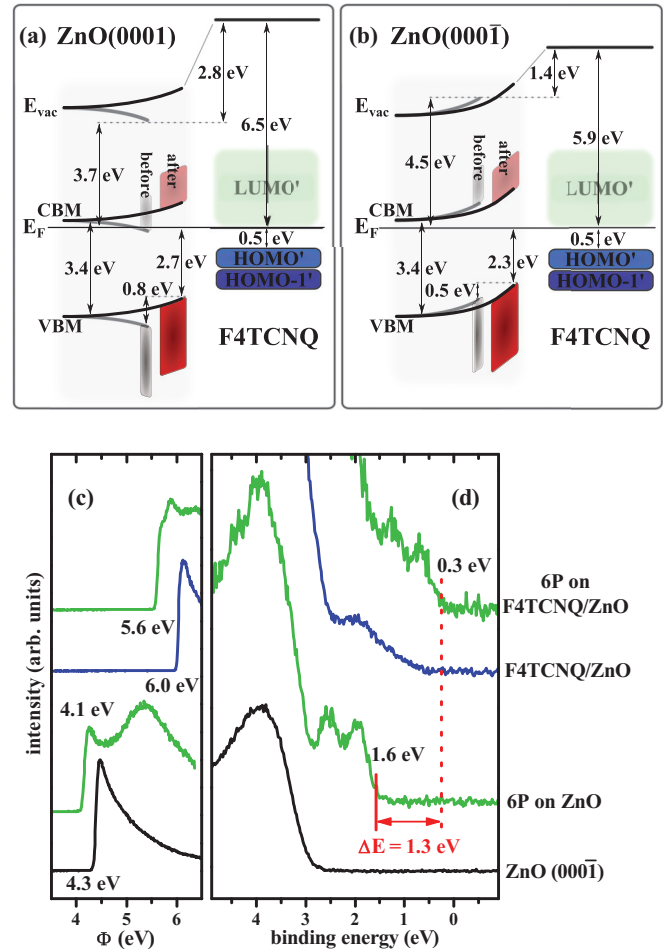


FIG. 5. (Color online) Energy-level diagrams for the adsorption of F4TCNQ on (a) ZnO(0001) and (b) ZnO(000-1). Gray shades indicate the energy levels in ZnO before F4TCNQ adsorption. HOMO', HOMO-1', and LUMO' indicate the energy levels of F4TCNQ in the adsorbed state as derived from the photoemission measurements. (c) SECO and (d) valence region UPS spectra for 6P deposited on bare and F4TCNQ-modified ZnO(000-1) as indicated in the figure.

Finally, the spectra of Figs. 5(c) and 5(d) demonstrate that the energy-level alignment at a ZnO/organic semiconductor [here: *p*-sexiphenyl (6P), a blue light emitter] interface can be substantially altered by insertion of an F4TCNQ interlayer and its induced $\Delta\Phi$. Although the low-binding energy onset of emission from the 6P HOMO level is at 1.6 eV on pristine ZnO(000-1), it is at 0.3 eV when F4TCNQ precovers the inorganic surface. Assuming that the work-function changes upon 6P deposition on both surfaces are caused by changes in the ZnO surface band bending, the energy offset between the ZnO valence-band maximum and the 6P HOMO onset increases from 1.5 eV (pristine) to 2.4 eV (with F4TCNQ). This documents a substantial functionality expansion of inorganic/organic heterojunctions in optoelectronic devices since surface band-bending-related work-function changes in inorganic semiconductors alone cannot reliably be used to change the heterojunction-level alignment.²²

IV. CONCLUSION

To summarize, we demonstrated that the work function of the two polar surfaces of ZnO can be controlled over wide ranges (up to 2.8 eV) by adsorbing the molecular electron acceptor F4TCNQ in the (sub-) monolayer regime. Although this is phenomenologically similar to what was observed for metal surfaces, the mechanism of the Φ increase differs markedly for the inorganic semiconductor. Simple electrostatic considerations show that $\Delta\Phi$ relies on two complementary mechanisms due to electron transfer to the surface-adsorbed acceptor, i.e., band bending in the inorganic semiconductor and an interface dipole, yielding $\Delta\Phi_{\text{BB}}$ and $\Delta\Phi_{\text{ID}}$, respectively. Noteworthy, we find that at low-doping levels of the semiconductor $\Delta\Phi_{\text{BB}}$ is the dominating contribution to the overall work

function change and that *minute electron transfer* (in the range of 0.02 e/molecule in our case) *is sufficient to induce significant* $\Delta\Phi$. Consequently, in addition to the acceptor electron affinity, the semiconductor-bulk-doping level is a key parameter to control (i) Φ and (ii) the charge state of the adsorbed acceptor layer. This has important implications for adjusting the energy levels at organic/inorganic heterojunctions and their (opto-) electronic functionality as shown here for ZnO and 6P.

ACKNOWLEDGMENT

This work was supported by the SFB951 (DFG). Y.X. acknowledges support of the Alexander von Humboldt Foundation.

-
- ¹H. Ishii, K. Sugiyama, E. Ito, and K. Seki, *Adv. Mater.* **11**, 605 (1999).
- ²S. R. Day, R. A. Hatton, M. A. Chesters, and M. R. Willis, *Thin Solid Films* **410**, 159 (2002).
- ³H. Glowatzki, B. Bröker, R.-P. Blum, O. T. Hofmann, A. Vollmer, R. Rieger, K. Müllen, E. Zojer, J. P. Rabe, and N. Koch, *Nano Lett.* **8**, 3825 (2008).
- ⁴N. Koch, S. Duhm, J. P. Rabe, A. Vollmer, and R. L. Johnson, *Phys. Rev. Lett.* **95**, 237601 (2005).
- ⁵L. Romaner, G. Heimel, J. L. Brédas, A. Gerlach, F. Schreiber, R. L. Johnson, J. Zegenhagen, S. Duhm, N. Koch, and E. Zojer, *Phys. Rev. Lett.* **99**, 256801 (2007).
- ⁶G. M. Rangger, O. T. Hofmann, L. Romaner, G. Heimel, B. Bröker, R.-P. Blum, R. L. Johnson, N. Koch, and E. Zojer, *Phys. Rev. B* **79**, 165306 (2009).
- ⁷W. Gao, and A. Kahn, *Org. Electron.* **3**, 53 (2002).
- ⁸V. E. Henrich and P. A. Cox, *The Surface Science of Metal Oxides* (Cambridge University Press, New York, 1994).
- ⁹M. Breendon, M. J. S. Spencer, and I. Yarovsky, *Surf. Sci.* **603**, 3389 (2009).
- ¹⁰W. Chen, D. Qi, X. Gao, and A. T. S. Wee, *Prog. Surf. Sci.* **84**, 279 (2009).
- ¹¹S. Blumstengel, S. Sadofev, H. Kirmse, and F. Henneberger, *Appl. Phys. Lett.* **98**, 031907 (2011).
- ¹²See Supplemental Material at <http://link.aps.org/supplemental/10.1103/PhysRevB.87.155311> for O1s and Zn3p core-level spectra.
- ¹³O. Dulub, U. Diebold, and G. Kresse, *Phys. Rev. Lett.* **90**, 016102 (2003).
- ¹⁴M. Valtiner, M. Todorova, G. Grundmeier, and J. Neugebauer, *Phys. Rev. Lett.* **103**, 065502 (2009).
- ¹⁵B. Meyer, *Phys. Rev. B* **69**, 045416 (2004).
- ¹⁶S. T. King, S. S. Parihar, K. Pradhan, H. T. Johnson-Steigelman, and P. F. Lyman, *Surf. Sci.* **602**, L131 (2008).
- ¹⁷S. Braun and W. R. Salaneck, *Chem. Phys. Lett.* **438**, 259 (2007).
- ¹⁸D. Qi, W. Chen, X. Gao, L. Wang, S. Chen, K. P. Loh, and A. T. S. Wee, *J. Am. Chem. Soc.* **129**, 8084 (2007).
- ¹⁹W. Chen, S. Chen, D. C. Qi, X. Y. Gao, and A. T. S. Wee, *J. Am. Chem. Soc.* **129**, 10418 (2007).
- ²⁰C. Coletti, C. Riedl, D. S. Lee, B. Krauss, L. Patthey, K. von Klitzing, J. H. Smet, and U. Starke, *Phys. Rev. B* **81**, 235401 (2010).
- ²¹W. Mönch, *Semiconductor Surfaces and Interfaces*, 3rd ed., edited by G. Ertl, R. Gomer, H. Lüth, and L. Mills, Springer Series in Surface Science, Vol. 26 (Springer, Berlin/Heidelberg/New York, 2001).
- ²²Y. Gassenbauer and A. Klein, *J. Phys. Chem. B* **110**, 4793 (2006).